Two-Dimensional Markov Chain Analysis of Radiation-Induced Soft Errors in Subthreshold Nanoscale CMOS Devices

Pooya Jannaty, Florian C. Sabou, Matthew Gadlage, R. Iris Bahar, Joseph Mundy, William Patterson, Robert A. Reed, *Senior Member, IEEE*, Robert A. Weller, Ronald D. Schrimpf, and Alexander Zaslavsky

***Abstract*—Radiation-induced soft errors have been a reliability concern for logic integrated circuits since their emergence. Feature-size and supply-voltage reduction require the analysis of soft-error sensitivity as a function of technology scaling. In this paper, an analytical framework based on Markov chains and queue theory is presented for computation of alpha-particle-induced soft-error rates of a flip-flop operated in the subthreshold regime. The proposed framework is capable of reflecting the technology parameters such as supply voltage V_{dd}, channel length, process-induced threshold variation, and operating temperature. As an example, the framework is used to investigate the mean time to error of flip-flops built in a 32 nm fully-depleted silicon-on-insulator technology operating in the subthreshold regime subject to two limiting fluxes of alpha particle radiation: high at 100 $(\alpha/\mathrm{h.cm}^2)$ and ultra-low alpha (ULA) emission 0.002 $(\alpha/\mathrm{h.cm}^2)$.**

***Index Terms*—Alpha-particle radiation effects, CMOS devices, logic devices, radiation effects in devices, reliability, single event upset, soft errors, SRAMs.**

I. Introduction

INTEREST in ultra-low-voltage digital circuits has been growing in the past years, prompted by the need to reduce the overall energy consumption [1], [2]. If the power reduction requirement is particularly stringent in some specific application, such as biomedical implants, environmental-monitoring devices or space systems, reducing V_{dd} into the subthreshold regime could prove useful [3], [4]. This reduction in the operating voltage raises the need for probabilistic frameworks capable of analyzing the effect of noise sources on low-power devices. The error rate estimates arising from such models can serve as a guideline for designing logic circuits operated at ultra-low or subthreshold V_{dd}.

Manuscript received March 27, 2010; revised June 09, 2010; accepted August 04, 2010. Date of publication October 04, 2010; date of current version December 15, 2010. The work at Brown was supported in part by NSF NIRT award CCF-0506732, NSF award ECCS-0701635, and by the Defense Threat Reduction Agency, Basic Research Award HDTRA1-10-1-0013. The work at Vanderbilt was supported by AFOSR through the MURI program and by the Defense Threat Reduction Agency, Basic Research Award HDTRA1-10-1-0013.

P. Jannaty, F. C. Sabou, R. I. Bahar, J. Mundy, W. Patterson, and A. Zaslavsky are with the Department of Physics and the School of Engineering, Brown University, Providence, RI 02912 USA (e-mail: pooya@brown.edu).

M. Gadlage, R. A. Reed, R. A. Weller, and R. D. Schrimpf are with the Department of Electrical Engineering and Computer Science, Vanderbilt University, Nashville, TN 37235 USA.

Color versions of one or more of the figures in this paper are available online at http://ieeexplore.ieee.org.

Digital Object Identifier 10.1109/TNS.2010.2068561

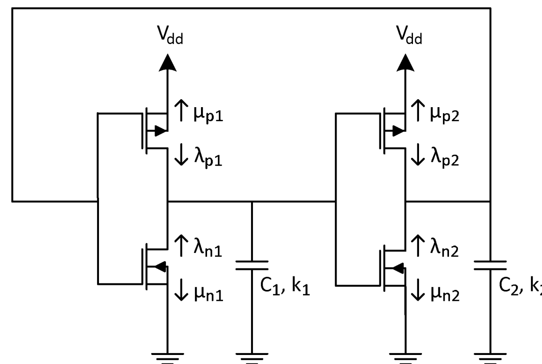

Fig. 1. The modeled flip-flop circuit. Capacitors C_1 and C_2 represent the node capacitances associated with each inverter. For each transistor, the charging and discharging rates λ and μ determine the electron populations on the node capacitances.

In our previous work [5]–[7], a probabilistic framework for the analysis of thermal-noise-induced variations in the logic stability of memory circuits such as flip-flops has been developed. As shown in Fig. 1, noise in a flip-flop operated in the subthreshold regime can be represented as a Poisson process with independent distributions for the arrival and departure of carriers at a drain or source node [8]. The node-capacitor charge is modeled as a queue where the transistor current fluctuations are considered to be random carrier arrival and departure events. The result is a two-dimensional (2D) queue that contains all the available states for the system considered in terms of the number of electrons k_1, k_2 on the two inverters.

The two valid logic states, '0' and '1', correspond to states in opposite corners of the 2D queue. Considering only the effects of thermal noise, previous work [5], [6] has shown that thermally-induced transitions between the stable states are exponentially rare and occur predominantly on a diagonal path between the stable corner states. Recently we have generalized our approach to a numerical solution of the full 2D queue [7]. As described in the next section, radiation events create a wide range of charge amounts at either electronic node. This sudden change in the electron population on the two inverters also changes the state of the system as represented in the 2D queue, often moving the system far from the stable corner states. The cumulative effects of the thermal broadening of the logic states and radiation render all states in the 2D queue to have a non-negligible transient occupation probability. Therefore, a complete solution of the full 2D queue is required to investigate the soft-error rates induced by radiation.

The paper is organized as follows: Section II details the simulation process for the alpha particle radiation. Section III briefly reviews the formulation for the 2D Markov chain (fully described in [7]). Section IV presents the soft error rates for the modeled flip-flop. Finally, Section V contains the conclusions.

II. Alpha Particle Radiation

The interaction of alpha particles with semiconductor devices can have a significant impact on electronic system reliability. Alpha particles can be emitted by trace impurities (such as uranium) in packaging materials [9], and can be byproducts of neutrons produced by cosmic radiation [10]. An ionizing particle, such as an alpha particle, can induce what is known as a single-event upset (SEU)—a change in the state of a node due to a single ionizing event. An alpha particle depositing charge in an SRAM cell and causing the bit to flip is a classic example of an SEU. As integrated circuits (ICs) shrink in feature size, the charge needed to cause an SEU also decreases, and as a result, single events are projected to become one of the biggest reliability issues for advanced electronics.

Charge generated by an alpha particle has to be collected at a circuit node to cause an SEU. For the radiation simulations in this paper, the volume in which charge can be collected is approximated as the body of the fully-depleted silicon-on-insulator (FD-SOI) device. This technology was chosen for analysis since the charge-collection volumes are relatively simple and it also holds the promise to become a mainstream technology for general applications. For the simulations in this paper, we used a 32 nm FD-SOI technology described in [11] with an effective gate length $L_G \sim 25$ nm and Si channel thickness of 10 nm.

To gain insight into the amount of charge an alpha particle can generate in a highly-scaled FD-SOI SRAM cell, simulations were performed using the Monte Carlo radiative energy deposition (MRED) software [12]. MRED is a simulation tool, based on the Geant4 libraries [13], for quantifying the energy deposited by radiation in microelectronic devices. A $10^4\ \mathrm{nm} \times 10^4\ \mathrm{nm} \times 7 \cdot 10^2\ \mathrm{nm}$ silicon block was simulated for a range of sensitive volumes, as seen in Fig. 2. The sensitive volume (representing the volume for which charge is collected, as described above) is the region in which the deposited energy is recorded by the MRED simulation and corresponds to the channel region of one transistor in the FD-SOI SRAM cell.

The average charge generated in the sensitive volume is plotted versus incident particle energy in Fig. 3 for 1.3×10^9 alpha particles normally incident on the top of the silicon block. The charge generated in the sensitive volume is obtained from the MRED simulations based on the average energy needed to create an electron hole pair in silicon ($\sim$ 3.6 eV at room temperature). If the width of a transistor in an FD-SOI SRAM doubles, the area under the gate (i.e., the body region) also doubles. Therefore, for a given particle fluence, the number of alpha particles that deposit energy in the body increases proportionally. To confirm this, the sensitive volume was increased from $25\ \mathrm{nm} \times 25\ \mathrm{nm} \times 10\ \mathrm{nm}$ to $200\ \mathrm{nm} \times 25\ \mathrm{nm} \times 10\ \mathrm{nm}$. The simulations for 5 MeV alpha particles in Fig. 2 show that the number of events scales linearly with the size of the sensitive volume. This property will be used later when transistors with larger sensitive volumes are analyzed, both for normal and isotropic alpha particle incidence.

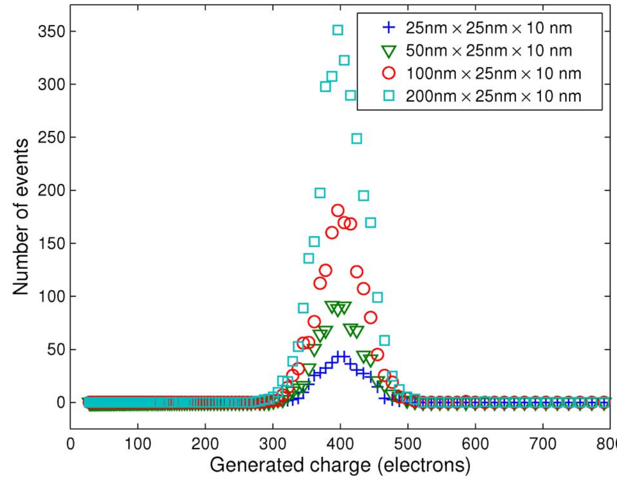

Fig. 2. Number of events observed for four different sensitive volumes corresponding to different transistor widths W, with gate length and channel thickness fixed. The number of events observed scales linearly with the width of the sensitive volume.

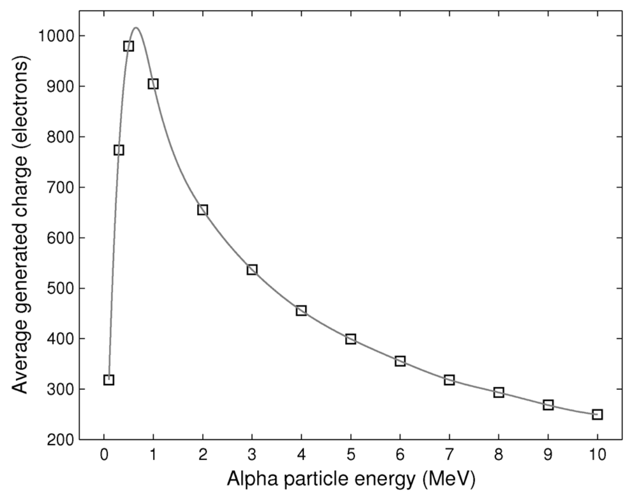

Fig. 3. Average charge generated in the sensitive volume as a function of the incident alpha particle energy for normally-incident particles.

III. Formulation of Two-Dimensional Markov Chain

In this section, an outline of the probabilistic formulation of a 2D Markov chain is presented. Both the steady-state and transient behavior of the system are formulated in terms of probability density functions (PDFs) and the results are used in Section IV.

For generality, a 2D chain of $N+1$-by-$N+1$ states, extending from the stable state $(N, 0)$ to the other stable state $(0, N)$ is assumed, see Fig. 4, where state (m, n) corresponds to the flip-flop having $k_1 = m$ electrons on one inverter and $k_2 = n$ electrons on the other. The rates of transmission from any state to its adjacent states are given in 4 matrices of the same size named $\mathbf{u}$, $\mathbf{d}$, $\mathbf{r}$ and $\mathbf{l}$, for up, down, right and left, respectively.

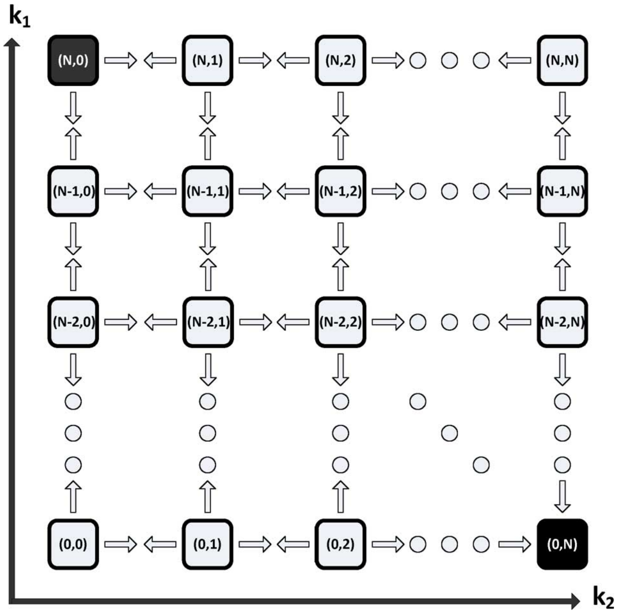

Fig. 4. Two dimensional Markov chain where state (m,n) corresponds to the flip-flop having $k_1 = m$ electrons on one inverter and $k_2 = n$ electrons on the other. The two stable states of the flip-flop are $(N,0)$ and $(0,N)$.

A. *Calculating the Mean Time to Failure Due to Thermal Fluctuations*

As mentioned earlier, in the subthreshold regime, the random sources governing the transitions have Poisson distributions, having their mean equal to the corresponding transition rates [8]. Associated to each state (m,n) are four independent Poisson sources for each main direction with the corresponding rates of $u_{m,n}$, $d_{m,n}$, $r_{m,n}$ and $l_{m,n}$, generating events according to their respective means. They can be written as

$$P_{iu0}(t) = \text{Prob(going up independently)}/dt = ue^{-ut} \quad (1)$$

and similar equations for moving in the other three directions.

For the system to move to, say, the upper state at time t, firstly, an 'up' event should happen, secondly, no other events, namely 'down', 'right' or 'left' should have happened until time t. This can be written mathematically as

$$\begin{aligned} P_{iu}(t) &= \text{Prob('up' event|no other events until time t)}/dt \\ &= P_{iu0}(t)\left(1-\int_0^t P_{id0}(t')dt'\right) \\ &\quad \times \left(1-\int_0^t P_{ir0}(t')dt'\right)\left(1-\int_0^t P_{il0}(t')dt'\right) \\ &= ue^{-(u+d+r+l)t}. \end{aligned} \quad (2)$$

For an arbitrary direction x, one has

$$P_{ix}(t) = xe^{-(u+d+r+l)t}, \quad x = u,d,r,l. \quad (3)$$

The transit time from the state (m,n) to the final state can be represented as the sum of transit time to an adjacent state and transit time from there to the final state. The sum of two transit times multiplied by their joint probability, integrated over all possible values for them, applied for all directions, gives the mean transit time:

$$T_{m,n} = \sum_{x=u,d,r,l} \int_0^\infty\int_0^\infty (t_{ix}+t_{xf})P_{ixf}(t_{ix},t_{xf})dt_{ix}dt_{xf} \quad (4)$$

where t_{ix} is the transit time from the initial state to the neighbor state x and t_{xf} is the transit time from the neighbor state x to the final state or sink. The index (m,n) is implicit in all variables although dropped for better readability.

By the definition of a Markov chain, the probability distribution for t_{xf} is independent of t_{ix}, since the system has no memory of which path it has taken so far. As a result:

$$T_{m,n} = \sum_{x=u,d,r,l} \int_0^\infty\int_0^\infty (t_{ix}+t_{xf})P_{ix}(t_{ix})P_{xf}(t_{xf})dt_{ix}dt_{xf} \quad (5)$$

As described in [7], (5) can be solved using a recursive approach, which reduces the memory requirements and the computation time significantly. Starting from the bottom-right corner in the 2D queue, $T_{0,N}$ is expressed in terms of the transit times of the preceding diagonal, $T_{1,N}$ and $T_{0,N-1}$. The transit times of this diagonal are in turn expressed in terms of those of the next diagonal, and so on, until all the diagonals are recursively scanned and the other corner of queue is reached. Once the value of $T_{N,0}$ is determined, it can be back-substituted into the recursive equations derived, until the values for all the transit times are calculated.

B. *Steady-State Thermal Distribution*

The same numerical approach introduced in [7] can be used to derive the steady-state thermal distribution of a 2D system. This distribution will be used later in estimating the radiation-induced soft-error rates in a flip-flop.

Given an initial probability distribution for the states of the system, the continuity equation governs the dynamics of probability flow between the states:

$$-\alpha\frac{\partial P^{ss}_{m,n}(t)}{\partial t} = (\nabla\cdot rP^{ss}(t))|_{m,n} \quad (6)$$

in which α is a constant of proportionality and $rP^{ss}(t)$ indicates the net probability flow out of the state (m,n). As $t\to\infty$ the system acquires a global steady state and the probabilities lose their time dependence, making the left hand side of (6) zero. In this condition, expanding the discrete divergence in the right hand side of the same equation reads

$$\begin{aligned}(u_{m,n}+d_{m,n}+r_{m,n}+l_{m,n})P^{ss}_{m,n} &= d_{m+1,n}P^{ss}_{m+1,n} \\ &+u_{m-1,n}P^{ss}_{m-1,n}+l_{m,n+1}P^{ss}_{m,n+1}+r_{m,n-1}P^{ss}_{m,n-1}. \end{aligned} \quad (7)$$

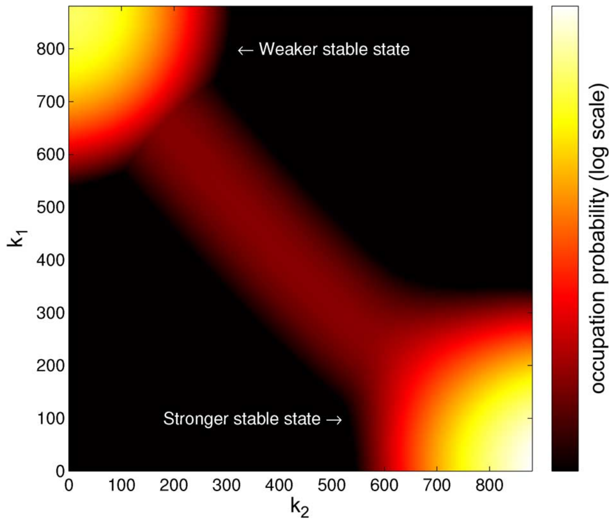

Fig. 5. The process-induced threshold variations in the transistors that make up the flip-flop render a given logic state to be more stable than the other. Steady-state thermal broadening for an FD-SOI CMOS flip-flop operated at $V_{dd} = 0.3$ V illustrates the confining of the system within the well defined logic states and exponentially rare transitions. The x and y axes map the 2D queue, while the color axis presents the log-scale numerical results for the occupation probability.

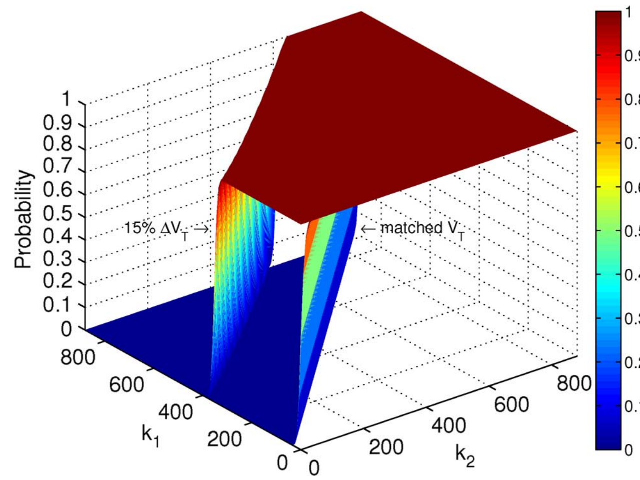

Fig. 6. Transient collapse probability for FD-SOI CMOS flip-flops with matched and 15% mismatched V_T, operated at $V_{dd} = 0.3$ V. Starting from any state (m, n) on the 2D queue, the height indicates the probability for the system to collapse to the state (0, 900). The probability of collapse to the state (900, 0) is the 1-complement of this value.

Eq. (7) applied to all the states within a 2D queue produces a system of equations which can be solved using the same techniques described in [7].

The thermal distribution for an FD-SOI CMOS flip-flop with 15% threshold variation is shown in Fig. 5 [14]. Because of the asymmetry in the device resulting from the threshold variation, the device is more likely to be found in the stronger stable state than in the weaker stable state, if we let the device run indefinitely without applying an input. In this particular case, the probability of the circuit making a transition from one stable state to the other due only to the effects of thermal noise is negligible. The importance of the analysis is that it allows the effects of larger fluctuations, such as those introduced by radiation effects, to be quantified in a way that includes variations in the operating point due thermal fluctuations. This is used in Section IV.

C. System Transient Behavior

Given a perturbation to the system, for example due to an incident alpha particle, the system changes its state abruptly, most likely to a state away from the two stable states. Such a volatile system will eventually relax to either of its stable states via a transient route on the 2D queue. Depending on the strength of the initial perturbation and the probabilistic nature of the system in responding to it, the final state might not be identical to the initial one, leading to a soft error. It is desired to know the probability of collapse to either of the stable states, given an arbitrary initial state anywhere on the 2D queue. The equations to be solved are

$$P^{tr}_{m,n} = z_{m,n}\left(u_{m,n}P^{tr}_{m+1,n} + d_{m,n}P^{tr}_{m-1,n} + l_{m,n}P^{tr}_{m,n-1} + r_{m,n}P^{tr}_{m,n+1}\right) \quad (8)$$

where $P^{tr}_{m,n}$ denotes the probability of collapse to the state $(0, N)$, let the system initiate from the state (m, n). The probability of collapse to the state $(N, 0)$ is $1 - P^{tr}_{m,n}$ for obvious reasons. Eq. (8) can be solved using the same technique described in [7].

The algebraic nature of the computational framework makes it possible to quantify the effects of important varying parameters such as the manufacturing-process-induced threshold variations of devices in integrated circuits. The variations in the threshold voltage for cutting edge technologies are approximately 10–15% of the nominal V_T [14]. The method described here accounts for such threshold variations by adjusting the transition rates between neighboring states to reflect the mismatch between the transistors in the flip-flop. To mirror the known spread in threshold voltage variations, FD-SOI CMOS flip-flops with perfectly matched and 15% mismatched V_T have been investigated and the results are shown in Fig. 6. It can be observed that threshold variations have an important effect in determining the stability domains for given devices with respect to transient perturbations, such as the ones created by alpha particle strikes.

The sharp switching staircase in Fig. 6 reflects the probability domains for single flip-flops with a mismatch of either zero or 15% in V_T between the inverters. For a large ensemble of devices, the distribution of threshold voltage variations would lead to a smoother average switching probability curve falling between the extreme cases illustrated in Fig. 6.

IV. Estimating Radiation-Induced Soft Error Rates

Equipped with the solutions for probability moment distributions, as well as the steady-state and transient behavior of the 2D system for each of its individual states, a systematic approach for a first-order estimation of the PDF of failure for a flip-flop under radiation is established in this section.

Assume that the function $event(q)$ contains the number of single particle events out of N_{inc} incident particles, as a function of deposited charge q on a sensitive volume as discussed in previous sections. If the flip-flop system is in state (m,n) not far from $(N,0)$ and some charge q is deposited on its first capacitive inverter, then the system moves to the state $(m+q,n)$. Therefore the probability for the system to relax to the state $(0,N)$, leading to a soft error, is equal to $P^{tr}_{m+q,n}$ which is previously obtained as the solution of (8). This probability, averaged on the two inverters, times $event(q)$, integrated over charge q, times the steady-state probability $P^{ss}_{m,n}$, summed over all the states (m,n) with condition $m+n<N$, gives the number of soft-error events due to N_{inc} incident particles. This number divided by N_{inc}, gives the probability for a single particle to cause an error:

$$P_{single}=\frac{1}{N_{inc}}\sum_{m+n<N}P^{ss}_{m,n}\int_q\frac{P^{tr}_{m+q,n}+P^{tr}_{m,n+q}}{2}event(q)dq \tag{9}$$

Implicit in this equation is that the distribution $P^{ss}_{m,n}$ is renormalized over the states $m+n<N$.

Assuming that the radiation flux on a single device is known, the average time interval between two incident particles is $T=1/flux$. For a soft-error event to happen between the times t and $t+dt$, none of the t/T incident particles arriving before time t should cause any events, while the next particle arriving between the aforementioned interval, with probability dt/T, should cause an event. This, by definition, gives the time-dependent PDF for soft-error events in a power-law form:

$$P_{error}(t)=\frac{1}{T}P_{single}(1-P_{single})^{t/T}. \tag{10}$$

In obtaining (9) and (10), the following assumptions were made:

- Incident particles were assumed to arrive one at a time on a single device within a device relaxation time frame. This is a legitimate assumption for almost all practical purposes: even with a flux of 100 $(\mathrm{alpha/hour.cm^2})$, the average time between two arrivals on an area of 1 cm^2 is 36 seconds which is orders of magnitude larger than device relaxation times ($\sim$1 ns, [7]).
- In (9) it was assumed that the deposited charge will not cause the system to move beyond its available states. Mathematically, this means that q is always such that $0\le m+q\le N$ and $0\le n+q\le N$. For instances that this condition does not hold, the corresponding P^{tr} in (9) can be replaced by unity as a worst case scenario, to enforce a soft error. However, the violation of this condition is not a concern for the states (m,n) far from the stable state $(N,0)$ as the overall effect will be exponentially attenuated by the term $P^{ss}_{m,n}$ for such states.
- The detailed physics of charge deposition was ignored in the derivations above and it was assumed that all the charge deposited in the sensitive volume is collected by the device. This assumption is based on the fact that the sensitive volume coincides with the transistor channel.

To illustrate this method, consider the event-charge curves for alpha particles of different energies shown in Fig. 7. To obtain each of these curves, 10^8 alpha particles were incident on an area of 100 $\mu\mathrm{m}^2$ and only the fraction of charge deposited in a sensitive volume representing the transistor channel was recorded. All the curves in Fig. 7(a) correspond to normally-incident radiation whereas Fig. 7(b) compares the normally-incident and isotropically-incident radiation over 2π steradians, both for alpha particle energy of 5 MeV. Evident from Fig. 7(b) is that the isotropic radiation has a much wider distribution of generated charge.

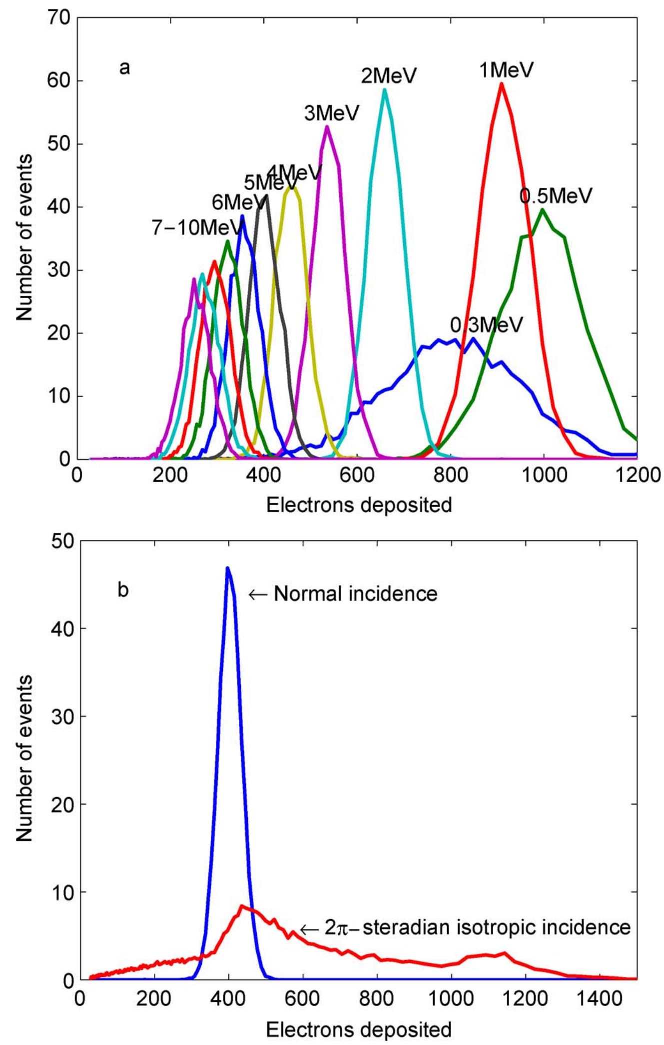

Fig. 7. Number of events depositing a given amount of charge due to 10^8 incident alpha particles of different energies. Only the amount of charge deposited in a sensitive volume representing the transistor channel was recorded. (a) normal-incidence radiation at different energies, (b) comparison between normally-incident and isotropically-incident 5 MeV alpha particles over 2π steradians.

The soft error rates for alpha particles with various incident energies are calculated and shown in Fig. 8 in units of failures in time (FITs)[1] for an FD-SOI CMOS flip-flop of gate length $L_G=25$ nm and W/L ratio of 15 for its NMOS transistors and 60 for its PMOS transistors (for matched current drive). At $V_{dd}=0.3$ V, such a flip-flop contains $\sim$1000 electrons. The error rates were calculated for two alpha particle fluxes, 100 $(\mathrm{alpha/hour.cm^2})$ and 0.002 $(\mathrm{alpha/hour.cm^2})$ [15], the latter being the onset of ultra low alpha (ULA) emission.

As Fig. 8 suggests, the error rates for incident alpha-particle energies less than 3 MeV are roughly constant and independent

[1]FIT is the number of failures in 1 billion device-operation hours.

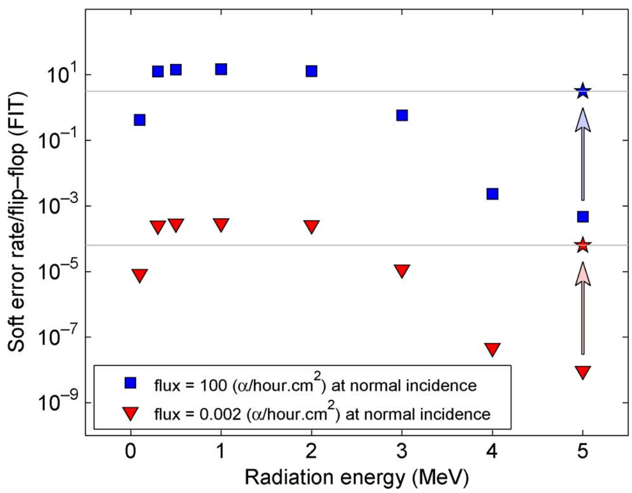

Fig. 8. Soft error rates measured in units of FIT for an FD-SOI CMOS flip-flop under radiation at normal (shown in squares and triangles) and 2π-steradian isotropic incidence (shown in stars), operated at $V_{dd} = 0.3$ V resulting in $\sim$1000 electrons.

of radiation energy. This is because the deposited charge at these energies is usually more than half the charge capacity of the flip-flop, see Fig. 3. Therefore, as illustrated in Fig. 6, almost all the incident particles will translate the system to the domain of the alternative stable state, causing a soft error. The mean time to failure becomes of the order of the average time between arrival of particles. For normally-incident alpha particles with energies greater than 3 MeV however, the number of particles that produce upsets is so small that their contribution to the FIT rate is negligible. However, in the case of isotropic radiation, the error rates are much higher, as shown in Fig. 8, due to the broader distribution of deposited charge.

The error rates presented in Fig. 8 agree with conventional analyses, which show that the radiation-induced soft error mechanism is strongly dominated by a critical charge collection value, at least for a simple system, like the flip-flop example used in this paper. The precise value of the critical collection threshold is influenced by several factors, such as device technology node and geometry, threshold variation, and operating voltage and temperature. Equally critical for the accurate prediction of radiation-induced soft errors is the correct evaluation of the interplay between the steady state, small thermal fluctuations that result in the broadening of the logic states, as illustrated in Fig. 5, and the large, transient fluctuations driven by the collected charge resulted after a radiation event. The computational framework presented in this paper, stemming from our previous work on thermal noise [5], [7], treats both fluctuation sources in a unified way.

V. Conclusion

In this paper, a probabilistic framework that has been applied in previous work to investigate the thermal-noise-induced soft errors has been extended to analyze the effects of radiation events on the logic stability of CMOS devices. While the thermal-induced variations have been shown in [5], [6] to be mostly confined to the diagonal region of the 2D queue, the electron population perturbations created by a particle strike span the entire 2D queue, which can be solved numerically [7].

As a predictive tool, the framework has been used to analyze the effects of alpha particle radiation on the logic stability of flip-flops built in a 32 nm silicon-on-insulator technology operating in the subthreshold regime. Two limiting values for the flux of alpha particle radiation have been considered: 100 $(\alpha/\mathrm{h.cm}^2)$ and ultra low alpha emission 0.002 $(\alpha/\mathrm{h.cm}^2)$. For high levels of normally-incident alpha particle radiation with incident energies below 4 MeV, the mean time to logic error is on the order of 10^{10} seconds. Considering the large number of memory devices on integrated circuits, such error rates, though small on an individual device basis, represent a significant reliability concern. For isotropically-incident alpha particles, higher energies are also problematic, due to the broader distribution of deposited charge.

References

[1] B. C. Paul, A. Raychowdhury, and K. Roy, "Device optimization for ultra-low power digital sub-treshold operation," in *Proc. Int. Symp. Low Power Electronics Design*, Aug. 2004, pp. 96–101.

[2] L. Chang, Y. Nakamura, R. K. Montoye, J. Sawada, A. K. Martin, K. Kinoshita, F. H. Gebara, K. B. Agarwal, D. J. Acharyya, W. Haensch, K. Hosokawa, and D. Jamsek, "A 5.3 GHz 8T-SRAM with operation down to 0.41 V in 65 nm CMOS," in *Proc. Symp. VLSI Circuits Digest of Technical Papers*, 2007, pp. 252–253.

[3] S. Hanson, B. Zhai, M. Seok, B. Cline, K. Zhou, M. Singhal, M. Minuth, J. Olson, L. Nazhandali, T. Austin, D. Sylvester, and D. Blaauw, "Exploring variability and performance in a sub-200-mV processor," *IEEE J. Solid-State Circuits*, vol. 43, no. 4, pp. 881–891, Apr. 2008.

[4] D. Bol, R. Ambroise, D. Flandre, and J. D. Legat, "Interests and limitations of technology scaling for subthreshold logic," *IEEE Trans. Very Large Scale Integr. (VLSI) Syst.*, vol. 17, no. 10, p. 1508, Oct. 2009.

[5] F. C. Sabou, D. Kazazis, R. I. Bahar, J. Mundy, W. R. Patterson, and A. Zaslavsky, "Markov chain analysis of thermally-induced soft errors in subthreshold nanoscale CMOS circuits," *IEEE Trans. Device Mater. Rel.*, vol. 9, no. 3, pp. 494–503, Sep. 2009.

[6] P. Jannaty, F. C. Sabou, R. I. Bahar, J. Mundy, W. R. Patterson, and A. Zaslavsky, "Numerical queue solution of thermal noise-induced soft errors in subthreshold CMOS devices," in *Proc. 20th Great Lakes Symp. VLSI*, 2010, pp. 281–286.

[7] P. Jannaty, F. C. Sabou, R. I. Bahar, J. Mundy, W. R. Patterson, and A. Zaslavsky, "Full two-dimensional Markov chain analysis of thermal soft errors in subthreshold nanoscale CMOS devices," *IEEE Trans. Device Mater. Rel.*, 2010, to be published.

[8] R. Sarpeshkar, T. Delbruck, and C. A. Mead, "White noise in MOS transistors and resistors," *IEEE Circuits Devices Mag.*, vol. 9, no. 6, pp. 23–29, Nov. 1993.

[9] R. C. Baumann, "Soft errors in advanced semiconductor devices-part I: The three radiation sources," *IEEE Trans. Device Mater. Rel.*, vol. 1, pp. 17–22, 2001.

[10] J. R. Letaw and E. Normand, "Guidelines for predicting single-event upsets in neutron environments RAM devices," *IEEE Trans. Nucl. Sci.*, vol. 38, no. 6, pp. 1500–1506, Dec. 1991.

[11] C. Fenouillet-Beranger, S. Denorme, B. Icard, F. Boeuf, J. Coignus, O. Faynot, L. Brevard, C. Buj, C. Soonekindt, J. Todeschini, J. C. Le-Denmat, N. Loubet, C. Gallon, P. Perreau, S. Manakli, B. Minghetti, L. Pain, V. Arnal, A. Vandooren, D. Aime, L. Tosti, C. Savardi, F. Martin, T. Salvetat, S. Lhostis, C. Laviron, N. Auriac, T. Kormann, G. Chabanne, S. Gaillard, O. Belmont, E. Laffosse, D. Barge, A. Zauner, A. Tarnowka, K. Romanjec, H. Brut, A. Lagha, S. Bonnetier, F. Joly, N. Mayet, A. Cathignol, D. Galpin, D. Pop, R. Delsol, R. Pantel, F. Pionnier, G. Thomas, D. Bensahel, S. Deleonibus, T. Skotnicki, and H. Mingam, "Fully-depleted SOI technology using high-k and single-metal gate for 32 nm node LSTP applications featuring 0.179 $\mu\mathrm{m}^2$ 6T-SRAM bitcell," in *Proc. IEDM Technical Digest*, Dec. 2007, pp. 267–270.

[12] K. M. Warren, R. A. Weller, M. H. Mendenhall, R. A. Reed, D. R. Ball, C. L. Howe, B. D. Olson, M. L. Alles, L. W. Massengill, R. D. Schrimpf, N. F. Haddad, S. E. Doyle, D. McMorrow, J. S. Melinger, and W. T. Lotshaw, "The contribution of nuclear reactions to heavy ion single event upset cross-section measurements in a high-density SEU hardened SRAM," *IEEE Trans. Nucl. Sci.*, vol. 52, no. 6, pp. 2125–2131, Dec. 2005.

[13] S. Agostinelliae, J. Allison, K. Amakoe, J. Apostolakisa, H. Araujoaj, P. Arcel, M. Asaig, D. Axeni, S. Banerjeebi, G. Barrandan, F. Behnerl, L. Bellagambac, J. Boudreaubd, L. Brogliaar, A. Brunengoc, H. Burkhardta, S. Chauviebj, J. Chumah, R. Chytraceka, G. Coopermanaz, G. Cosmoa, P. Degtyarenkod, A. Dell'Acquaa, G. Depaolay, D. Dietrichaf, R. Enamiab, A. Feliciellobj, C. Fergusonbh, H. Fesefeldtl, G. Folgera, F. Foppianoac, A. Fortias, S. Garelliac, S. Giania, R. Giannitrapanibo, D. Gibinm, J. J. Gómez Cadenasm, I. Gonźlezq, G. Gracia Abriln, G. Greeniausp, W. Greineraf, V. Grichinef, A. Grossheimm, S. Guatelliad, P. Gumplingerh, R. Hamatsubk, K. Hashimotoab, H. Hasuiab, A. Heikkinenah, A. Howardaj, V. Ivanchenkoa, A. Johnsong, F. W. Jonesh, J. Kallenbachaa, N. Kanayai, M. Kawabataab, Y. Kawabataab, M. Kawagutiab, S. Kelnerat, P. Kentr, A. Kimuraay, T. Kodamaaw, R. Kokoulinat, M. Kossovd, H. Kurashigeam, E. Lamannaw, T. Lampénah, V. Laraa, V. Lefeburel, F. Leibh, M. Liendll, W. Lockmanj, F. Longobm, S. Magnik, M. Maireao, E. Medernacha, K. Minamimotoaw, P. Mora de Freitasap, Y. Moritae, K. Murakamie, M. Nagamatuaw, R. Nartallob, P. Nieminenb, T. Nishimuraab, K. Ohtsuboab, M. Okamuraab, S. O'Neales, Y. Oohatabk, K. Paechaf, J. Perlg, A. Pfeiffera, M. G. Piaad, F. Ranjardn, A. Rybinak, S. Sadilova, E. Di Salvoc, G. Santinbm, T. Sasakie, N. Savvasas, Y. Sawadaab, S. Schereraf, S. Seiaw, V. Sirotenkoi, D. Smithg, N. Starkovf, H. Stoeckeraf, J. Sulkimoah, M. Takahataay, S. Tanakabg, E. Tcherniaeva, E. Safai Tehranig, M. Tropeanoae, P. Truscottbe, H. Unoaw, L. Urbanv, P. Urbanaq, M. Verderiap, A. Walkdenas, W. Wanderav, H. Weberaf, J. P. Wellischa, T. Wenausu, D. C. Williamsj, D. Wrightg, T. Yamadaaw, H. Yoshidaaw, and D. Zschiescheaf, "GEANT4-a simulation toolkit," *Nucl. Instrum. Methods Phys. Res. A*, vol. A506, pp. 250–303, 2003.

[14] H.-S. Wong, Y. Taur, and D. J. Frank, "Discrete random dopant distribution effects in nanometer-scale MOSFETs," *Microelectron. Reliab.*, vol. 38, no. 9, pp. 1447–1456, 1998.

[15] R. C. Baumann, "Radiation-induced soft errors in advanced semiconductor technologies," *IEEE Trans. Device Mater. Rel.*, vol. 5, no. 3, pp. 305–316, 2005.